Neuropsychopharmacology (2011) 36, 1021–1032

www.neuropsychopharmacology.org

Nicotine-Mediated Activation of Dopaminergic Neurons in Distinct Regions of the Ventral Tegmental Area

Rubing Zhao-Shea[1], Liwang Liu[1], Lindsey G Soll[1], Ma Reina Improgo[1], Erin E Meyers[2], J Michael McIntosh[3], Sharon R Grady[2], Michael J Marks[2], Paul D Gardner[1] and Andrew R Tapper*[,1]

[1]Department of Psychiatry, Brudnick Neuropsychiatric Research Institute, University of Massachusetts Medical School, Worcester, MA, USA; [2]Institute for Behavioral Genetics, University of Colorado, Boulder, CO, USA; [3]Departments of Psychiatry and Biology, University of Utah, Salt Lake City, UT, USA

Nicotine activation of nicotinic acetylcholine receptors (nAChRs) within the dopaminergic (DAergic) neuron-rich ventral tegmental area (VTA) is necessary and sufficient for nicotine reinforcement. In this study, we show that rewarding doses of nicotine activated VTA DAergic neurons in a region-selective manner, preferentially activating neurons in the posterior VTA (pVTA) but not in the anterior VTA (aVTA) or in the tail VTA (tVTA). Nicotine (1 μM) directly activated pVTA DAergic neurons in adult mouse midbrain slices, but had little effect on DAergic neurons within the aVTA. Quantification of nAChR subunit gene expression revealed that pVTA DAergic neurons expressed higher levels of α4, α6, and β3 transcripts than did aVTA DAergic neurons. Activation of nAChRs containing the α4 subunit (α4* nAChRs) was necessary and sufficient for activation of pVTA DAergic neurons: nicotine failed to activate pVTA DAergic neurons in α4 knockout animals; in contrast, pVTA α4* nAChRs were selectively activated by nicotine in mutant mice expressing agonist-hypersensitive α4* nAChRs (Leu9′Ala mice). In addition, whole-cell currents induced by nicotine in DAergic neurons were mediated by α4* nAChRs and were significantly larger in pVTA neurons than in aVTA neurons. Infusion of an α6* nAChR antagonist into the VTA blocked activation of pVTA DAergic neurons in WT mice and in Leu9′Ala mice at nicotine doses, which only activate the mutant receptor indicating that α4 and α6 subunits coassemble to form functional receptors in these neurons. Thus, nicotine selectively activates DAergic neurons within the pVTA through α4α6* nAChRs. These receptors represent novel targets for smoking-cessation therapies.
Neuropsychopharmacology (2011) **36,** 1021–1032; doi:10.1038/npp.2010.240; published online 2 February 2011

Keywords: dopamine; acetylcholine; nicotine; smoking; ventral tegmental area; mice

INTRODUCTION

Smoking is the primary cause of preventable mortality in the world (CDC, 2010). When volatilized, nicotine, the addictive component of tobacco smoke, is absorbed into the blood stream through the lungs and rapidly crosses the blood–brain barrier on the order of seconds (Tapper *et al*, 2006). In the CNS, nicotine targets and activates neuronal nicotinic acetylcholine (ACh) receptors (nAChRs), ligand-gated cation channels that, under normal conditions, are activated by the endogenous neurotransmitter, ACh (Albuquerque *et al*, 2009). A total of 12 mammalian genes encoding nAChR subunits have been identified (α2–α10 and β2–β4), and 5 subunits coassemble to form a functional receptor (Albuquerque *et al*, 2009). The majority of nAChRs with high affinity for agonists are heteromeric consisting of two or three α-subunits coassembled with two or three β-subunits, whereas a subset of low-affinity receptors are homomeric, consisting of predominantly α7 subunits (Albuquerque *et al*, 2009). The subunit composition of the receptor determines the biophysical and pharmacological properties of each receptor subtype. Thus, a vast array of nAChR subtypes exists.

Although nAChRs are expressed throughout the CNS, nicotine-induced activation of the mesocorticolimbic reward circuitry likely initiates addiction (Laviolette and van der Kooy, 2004). Within this pathway, nicotine ultimately drives the activity of dopaminergic (DAergic) neurons originating in the ventral tegmental area (VTA), resulting in increased DA release in the nucleus accumbens (NAc) and the prefrontal cortex, a phenomenon widely associated with drug reward or reinforcement (Dani, 2003). Various nicotinic receptor subtypes are widely expressed in the VTA in both DAergic projection neurons and local GABAergic interneurons (Champtiaux *et al*, 2002, 2003;

*Correspondence: Dr AR Tapper, Department of Psychiatry, Brudnick Neuropsychiatric Research Institute, University of Massachusetts Medical School, 303 Belmont Street, Worcester, MA 01604, USA, Tel: +1 508 856 2674, Fax: +1 508 856 2627, E-mail: Andrew.tapper@umassmed.edu
Received 10 November 2010; revised 7 December 2010; accepted 11 December 2010

Klink *et al*, 2001; Wooltorton *et al*, 2003). Several specific subunits have been identified that are critical for nicotine dependence-associated behaviors. Mice that do not express the $\beta2$ subunit fail to maintain nicotine self-administration, indicating that nAChRs containing $\beta2$ subunits (denoted by $\beta2^*$) are necessary for nicotine reinforcement (Picciotto *et al*, 1998). In addition, selective activation of $\alpha4^*$ nAChRs is sufficient for reward, tolerance, and sensitization (Tapper *et al*, 2004). Knockout (KO) mice that do not express $\beta2$, $\alpha4$, or $\alpha6^*$ nAChRs fail to self-administer nicotine but nicotine intake can be rescued by re-expressing these subunits into the VTA, thus highlighting the importance of this brain structure in nicotine reinforcement (Maskos *et al*, 2005; Pons *et al*, 2008).

Although the VTA consists of two predominant neuronal subtypes as discussed above, there is mounting evidence that suggests that this brain structure is not homogeneous but can be divided into discrete subregions, including anterior, posterior, and tail (Ikemoto *et al*, 1989; Ikemoto, 2007; Kaufling *et al*, 2009; Perrotti *et al*, 2005). Recent data have suggested that the anterior and posterior VTA (aVTA and pVTA, respectively) project to distinct regions of the striatum and are differentially responsive to various drugs of abuse, suggesting functional heterogeneity (Boehm *et al*, 2002; Ericson *et al*, 2008; Ikemoto *et al*, 2006; Shabat-Simon *et al*, 2008; Zangen *et al*, 2006). Importantly, rats will self-administer nicotine directly in the pVTA but not in the aVTA, although the mechanistic basis of this regional selectivity is unknown (Ikemoto *et al*, 2006).

The goal of this study was to determine whether nicotine, at rewarding doses, activates DAergic neurons within the VTA in a region-selective manner and to identify a mechanism that may account for this selectivity. Insights into nicotine-mediated activation of this important brain region will significantly contribute to understanding the molecular basis of nicotine addiction. In addition, identification of nAChR subtypes activated by physiologically relevant concentrations of nicotine will provide novel molecular targets for smoking-cessation therapeutics.

MATERIALS AND METHODS

Animals

Adult (aged 8–10 weeks), male C57BL/6J mice (Jackson Laboratory, West Grove, PA, USA), were used in experiments, in addition to Leu9′Ala heterozygous and $\alpha4$ KO homozygous mice as indicated. Leu9′Ala and $\alpha4$ KO lines have been back-crossed to the C57BL/6J strain for at least nine generations. The genetic engineering of the Leu9′Ala and $\alpha4$ KO line has been described previously (Ross *et al*, 2000; Tapper *et al*, 2004). Animals were housed four per cage up until the start of each experiment. They were kept on a standard 12-h light–dark cycle with lights on at 0700 hours and off at 1900 hours. Mice had access to food and water *ad libitum*. All experiments were conducted in accordance with the guidelines for care and use of laboratory animals provided by the National Research Council (1996), as well as with an approved animal protocol from the Institutional Animal Care and Use Committee of the University of Massachusetts Medical School or the University of Colorado.

Drugs

Nicotine hydrogen tartrate, mecamylamine hydrochloride, CNQX, atropine, and bicuculline methbromide (Sigma-Aldrich, St Louis, MO, USA) were dissolved in sterile saline or artificial cerebrospinal fluid (ACSF) as indicated. ACSF solution contained (in mM): 125 NaCl, 2.5 KCl, 1.2 $NaH_2PO_4 \cdot H_2O$, 1.2 $MgCl_2$ $6H_2O$, 2.4 $CaCl_2 \cdot 2H_2O$, 26 $NaHCO_3$, and 11 D-glucose. Nicotine doses are reported as nicotine-free base. Both α-conotoxin MII and α-conotoxin MII (E11A) were synthesized as described previously (McIntosh *et al*, 2004).

Immunofluorescence

Before the start of double-labeling experiments, all mice were administered an intraperitoneal (i.p.) injection of saline for 3 days to habituate them to handling and to exclude neuron activation due to stress. C57BL/6J mice ($n = 9$) were divided into three groups and received either a saline injection followed by a second saline injection, or a saline injection followed by a 0.5 mg/kg nicotine injection, or an injection of 3.0 mg/kg mecamylamine followed by a 0.5 mg/kg nicotine injection as indicated. The time between the first and second injection was 15 min. Ninety minutes after the second injection, all mice were deeply anesthetized with sodium pentobarbital (200 mg/kg, i.p.) and perfused transcardially with 10 ml ice-cold 0.1 M phosphate-buffered saline (PBS), followed by 10 ml ice-cold 4% (W/V) paraformaldehyde dissolved in 0.1 M PBS (pH 7.4). The brains were removed and processed for double immunolabeling as described previously (Hendrickson *et al*, 2009). For details, see Supplementary Materials and Methods.

Laser Capture Microdissection and Real-Time PCR for Measurement of nAChR Subunit Gene Expression

The brains were removed, snap frozen in dry ice-cooled 2-methylbutane ($-60^\circ C$), and stored at $-80^\circ C$. Coronal serial sections (10 μm) of the VTA were cut on a cryostat (Leica CM 3050s, Meyer Instrument, Houston, TX, USA) and affixed to uncoated, precleaned glass slides. Slides were rinsed with RNase Away (Invitrogen, Carlsbad, CA, USA) before usage to prevent RNA degradation. To further preserve RNA integrity, no tissue block was sectioned more than once and tissue was processed for laser capture microdissection (LCM) within 1 week of sectioning. A quick immunofluorescence staining protocol for TH was used to identify DA neurons. First, frozen sections were allowed to thaw for 30 s. Slides were immediately fixed in ice-cold acetone for 4 min. Slides were then washed in PBS, incubated with primary antibody mouse anti-TH (Santa Cruz Biotechnology, Santa Cruz, CA, 1 : 50 dilution for 10 min), washed in PBS once, followed by incubation in secondary fluorescent-labeled antibodies (Molecular Probes; goat anti-mouse Alex Fluor 594, 1 : 100) for 10 min. The slides were washed in PBS once, and then subsequently dehydrated in graded ethanol solution (30 s each in 70% ethanol, 95% ethanol, 100% ethanol, and once for 5 min in xylene). All antibodies were diluted in PBS, including 2% BSA and 0.2% Triton X-100. All PBS and dH_2O used were treated with diethylpyrocarbonate (DEPC)

for RNA preservation. The Veritas Microdissection System Model 704 (Arcturus Bioscience, Mountain View, CA, USA) was used for LCM. Spot sizes were set at 7.5–8.5 μm, power at 45 mW, and duration at 650 μs. Approximately 800–1400 TH-immunoreactive (TH-ir) neurons were cut in the region of the VTA in each animal ($n = 5$–7). Neurons were captured on CapSure Macro LCM caps (MDS Analytical Technologies, Sunnyvale, CA, USA). Total RNA was extracted from individual samples using RNAqueous—Micro (Micro Scale RNA Isolation kit, Ambion, Austin, TX, USA). Reverse transcription was performed using TaqMan Gene Expression Cells-to-CT kit (Ambion). PCR reactions were set up in 10 μl reaction volumes using TaqMan Gene Expression Master Mix and the TaqMan Gene Expression Assays for nAChR subunits. Glyceraldehyde-3-phosphate dehydrogenase (*GAPDH*) was used as an internal control gene. PCR was performed on neurons that were pooled for each animal in each brain region using an ABI PRISM 7500 Sequence Detection System, Version 1.4. Both no-template and no-reverse-transcriptase negative controls were performed. All reactions were performed in triplicate. Relative amplicon quantification was calculated as the difference between C_t values of *GAPDH* and that of the gene of interest ($-\Delta C_t$). Relative gene expression differences between groups of neurons were calculated using the $2^{-\Delta\Delta Ct}$ method.

Slice Preparation and Electrophysiological Recordings

Mice were deeply anesthetized with sodium pentobarbital (200 mg/kg, i.p.) and then decapitated. Their brains were quickly removed and placed in an oxygenated ice-cold high-sucrose ACSF (SACSF) containing kynurenic acid (1 mM, Sigma-Aldrich). Brain slices (180–200 μm) were cut using a Leica VT1200 vibratome (Leica Microsystem). The brain slices were incubated in oxygenated Earl's balanced salt solution supplemented with glutathione (1.5 mg/ml, Sigma-Aldrich), *N*-ω-nitro-L-arginine methyl ester hydrochloride (2.2 mg/ml, Sigma-Aldrich), pyruvic acid (11 mg/ml, Sigma-Aldrich), and kynurenic acid (1 mM) for 45 min at 34°C. Slices were transferred into oxygenated ACSF at room temperature for recording. SACSF solution contained (in mM): 250 sucrose, 2.5 KCl, 1.2 $NaH_2PO_4 \cdot H_2O$, 1.2 $MgCl_2 \cdot 6H_2O$, 2.4 $CaCl_2 \cdot 2H_2O$, 26 $NaHCO_3$, and 11 D-glucose. Single slices were transferred into a recording chamber that was continually superfused with oxygenated ACSF. The junction potential between the patch pipette and bath ACSF was nullified just before obtaining a seal on the neuronal membrane. Action potentials and currents were recorded at room temperature (22–24°C) using the whole-cell configuration of a Multiclamp 700B patch-clamp amplifier (Axon Instruments, Foster City, CA). Action potentials measured in a cell-attached mode were recorded at 31–32°C, and were obtained using a gap-free acquisition mode and Clampex software (Axon Instruments). I_h currents were elicited every 5 s by stepping from −60 mV to a test potential of −120 mV for 1 s using Clampex. Input resistances were calculated using steady-state currents elicited by 5-mV hyperpolarizing pulses. Signals were filtered at 1 kHz using the amplifier's four-pole, low-pass Bessel filter, digitized at 10 kHz with an Axon Digidata 1440A interface, and stored on a personal computer. Potential DAergic neurons were selected for recording, initially based on neuroanatomical region and soma shape. Action potential frequency (1–5 Hz) and I_h expression were also used for identification of neuronal identity. In addition, at the end of recording, the neuron cytoplasm was aspirated into the recording pipette and the contents were expelled into a microcentrifuge tube containing 75% ice-cold ethanol and stored at −20°C for at least 2 h before single-cell RT-PCR experiments to verify expression of TH. Overall, 91.3% of recorded neurons expressed TH (73/80) using the above-described criteria. Non-TH-expressing neurons ($n = 7$) were excluded from analysis. Pipette solution contained (in mM): 121 KCl, 4 $MgCl_2 \cdot 6H_2O$, 11 EGTA, 1 $CaCl_2 \cdot 2H_2O$, 10 HEPES, 0.2 GTP, and 4 mM ATP. The pipette solution was prepared using sterile-filtered DEPC-treated distilled water. Nicotine hydrogen tartrate (Sigma-Aldrich) was dissolved in distilled water. Drugs were applied to slices by gravity superfusion.

VTA Infusions

C57BL/6J animals were anesthetized with ketamine/xylazine (0.1 ml/10 g body weight, 10 mg/ml ketamine, 1 mg/ml xylazine). The surgical area was shaved and disinfected. Mice were placed in a stereotaxic frame (Stoelting, Wood Dale, IL, USA) using a mouse adaptor, and then a small incision was cut in the scalp to expose the skull. Using bregma and lambda as landmarks, the skull was leveled in the coronal and sagittal planes. For drug infusion, holes were drilled in the skull at the anteroposterior (AP, in reference to bregma) and the mediolateral (ML) coordinates that correspond to the pVTA (−3.4 mm AP, ± 0.5 mm ML) based on 'The Mouse Brain in Stereotaxic Coordinates' (Paxinos and Franklin, 2000). An injection syringe (Hamilton, Reno, NV) connected to a syringe pump (Stoelting Quintessential Stereotaxic Injector, Stoelting) was slowly lowered just dorsal to the pVTA, −3.9 mm from the skull and ACSF, or 100 nM α-conotoxin MII (E11A) was delivered at a constant volume of 0.133 μl/min. The injection needle was left in place for 5 min after each injection and then removed at a rate of 1 mm/min. Immediately after needle withdrawal, mice were injected i.p. with nicotine or saline. Mice were culled and their brains isolated for immunofluorescence 90 min after injection.

Data Analysis

Data were analyzed using two-way ANOVA with drug treatment and brain region as variables as indicated, followed by Bonferroni's *post hoc* tests. Data were analyzed using Graphpad Prism 5 software (Graphpad Software, La Jolla, CA, USA). Paired *T*-tests were used to analyze fold expression of qRT-PCR data. Results were considered significant at $p < 0.05$. All data are expressed as means ± SEM.

RESULTS

DAergic Neuron Size and Cell Density in the VTA

The VTA is not a homogeneous brain structure and can be divided into at least three distinct subregions, namely the aVTA, pVTA, and tail VTA (tVTA) according to their functional differentiation and projection targets (Kaufling

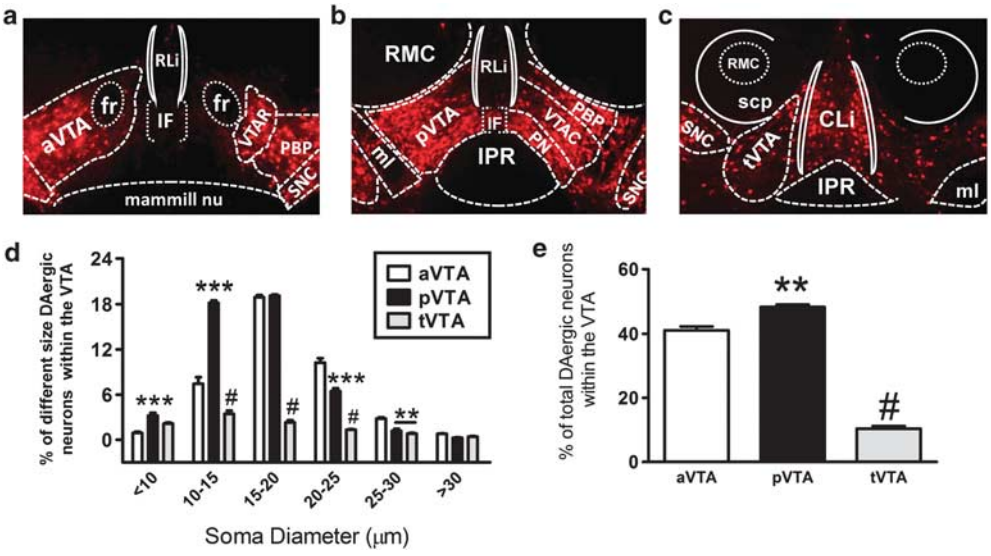

Figure 1 Definition, size, and density of DAergic neurons within the aVTA, the pVTA, and the tVTA. (a–c) Definitions of VTA subregions (Ikemoto, 2007; Kaufling *et al*, 2009; Paxinos and Franklin, 2000; Perrotti *et al*, 2005; Shabat-Simon *et al*, 2008). Representative midbrain slices containing the aVTA, pVTA, or tVTA. TH-ir neurons are labeled red. Brain region borders are outlined in white. (Panel a) aVTA (bregma from −2.92 to −3.28 mm): defined as the region dorsal to the medial mammillary nucleus and medial to the substantia nigra pars compacta (SNC). It contains two subregions: the ventral tegmental area rostral (VTAR) and the parabrachial pigmental area (PBP). The aVTA does not include midline nuclei such as the interfascicular nucleus (IF) and the rostral linear nucleus (RLi). A10 DAergic neurons located in the supramammillary nucleus described by Hokfelt *et al* (1984a, b) also are not included in the aVTA. (Panel b) pVTA (bregma from −3.28 to −3.80 mm): defined as the region dorsal to the interpeduncular nucleus (IPR), medial to the SNC and ventral to the red nucleus (RPC and/or RMC). It contains three subregions: the PBP, ventral tegmental area caudal (VTAC), and the paranigral nucleus (PN). The pVTA does not include the midline nuclei, such as the IF and the RLi and/or the caudal linear nucleus (CLi). A10 DAergic neurons located in the dorsal raphe nucleus described by Hokfelt *et al* (1984a, b) are not included in the pVTA. (Panel c) tVTA (bregma from −3.80 to −4.04 mm): defined as the most caudal extent of the VTA. Rostrally, the tVTA is limited to a subregion posterior to the PN and dorsolateral to the IP. More caudally, the position of the tVTA shifts dorsally and slightly laterally to become embedded within the superior cerebellar peduncle decussation (SCP). The tVTA has a low density of DAergic neurons and a high density of GABAergic neurons. The tVTA does not include the midline nuclei RLi or CLi. (Panel d) Quantification of DAergic neuron soma size in the aVTA (open bar), the pVTA (filled bar), and the tVTA (gray bar). Each bar represents the percentage of DAergic neurons with the indicated soma diameter (*x* axis in μm). (Panel e) Bar graph representation of DAergic neuron density in the aVTA, the pVTA, and the tVTA. In all, 2508–2864 DAergic neurons were measured per mouse ($n=3$). $^{**}p<0.01$, $^{***}p<0.001$ compared with that of aVTA. $^{\#}p<0.001$ compared with that of aVTA and pVTA.

et al, 2009; Perrotti *et al*, 2005; Rodd *et al*, 2004; Shabat-Simon *et al*, 2008). Figure 1 illustrates representative tyrosine hydoxylase-immunolabeled midbrain slices from each VTA subregion along with their precise description. To determine whether DAergic neurons within the aVTA, pVTA, and tVTA are morphologically distinct, we analyzed soma diameters in midbrain coronal sections from C57BL/6J mice. Somas were visualized by TH immunolabeling. The pVTA was anatomically recognized from the aVTA and tVTA by known landmarks (Shabat-Simon *et al*, 2008) and stereotaxic coordinates based on the mouse brain atlas of Paxinos and Franklin (2000) (Figure 1a–c). A total of 3301, 3877, and 832 TH-immunoreactive (TH-ir) neurons within the aVTA, pVTA, and tVTA, respectively, were measured from 3 mice. Neurons were classified into six groups based on diameter size (Figure 1d). Two-way ANOVA revealed that there was a significant main effect of brain region ($F_{2,36}=615.3$, $p<0.0001$), neuron size ($F_{5,36}=725.3.27$, $p<0.001$), and a significant brain region × neuron size interaction ($F_{10,36}=193.3$, $p<0.001$). The pVTA contained significantly more small DAergic neurons than did the aVTA or tVTA (ie, neurons smaller than 10–15 μm, Figure 1d). In contrast, there was a significantly greater percentage of large-size DAergic neurons located in the aVTA compared with the pVTA or tVTA (ie, neurons with soma diameter 20–30 μm, Figure 1d). In addition, analysis of the number of DAergic neurons per unit area (420 μm × 320 μm) indicated that there was a small but significantly greater density of TH-ir neurons in the pVTA than in the aVTA ($p<0.01$), whereas there were much fewer TH-ir neurons in the tVTA than in the aVTA and pVTA ($p<0.001$, Figure 1e).

Acute Nicotine Preferentially Activates DAergic Neurons within the pVTA

Previous studies have indicated that VTA subregions have different roles in modulating the rewarding properties of several drugs of abuse (Ikemoto, 2007; Ikemoto and Wise, 2002; Olson *et al*, 2005; Shabat-Simon *et al*, 2008). To determine whether nicotine preferentially activates the VTA in a subregion-selective manner, we challenged C57BL/6J mice with nicotine and counted the number of activated DAergic neurons in the aVTA, pVTA, and tVTA. Expression of the immediate early gene, *c-Fos*, was used as a measure of neuronal activation (Cole *et al*, 1989) and was analyzed in TH-ir neurons within the VTA by double-labeling immunofluorescence. Two-way ANOVA indicated that there was a significant main effect of brain region ($F_{8,54}=99.4$, $p<0.0001$), treatment ($F_{2,54}=444.4$, $p<0.001$), and a significant brain region × treatment interaction ($F_{16,54}=70.7$, $p<0.001$). Mice challenged with 0.5 mg/kg (i.p.) nicotine, a dose that conditions a place preference (ie, a 'rewarding' dose (Tapper *et al*, 2004)), exhibited a significant increase in

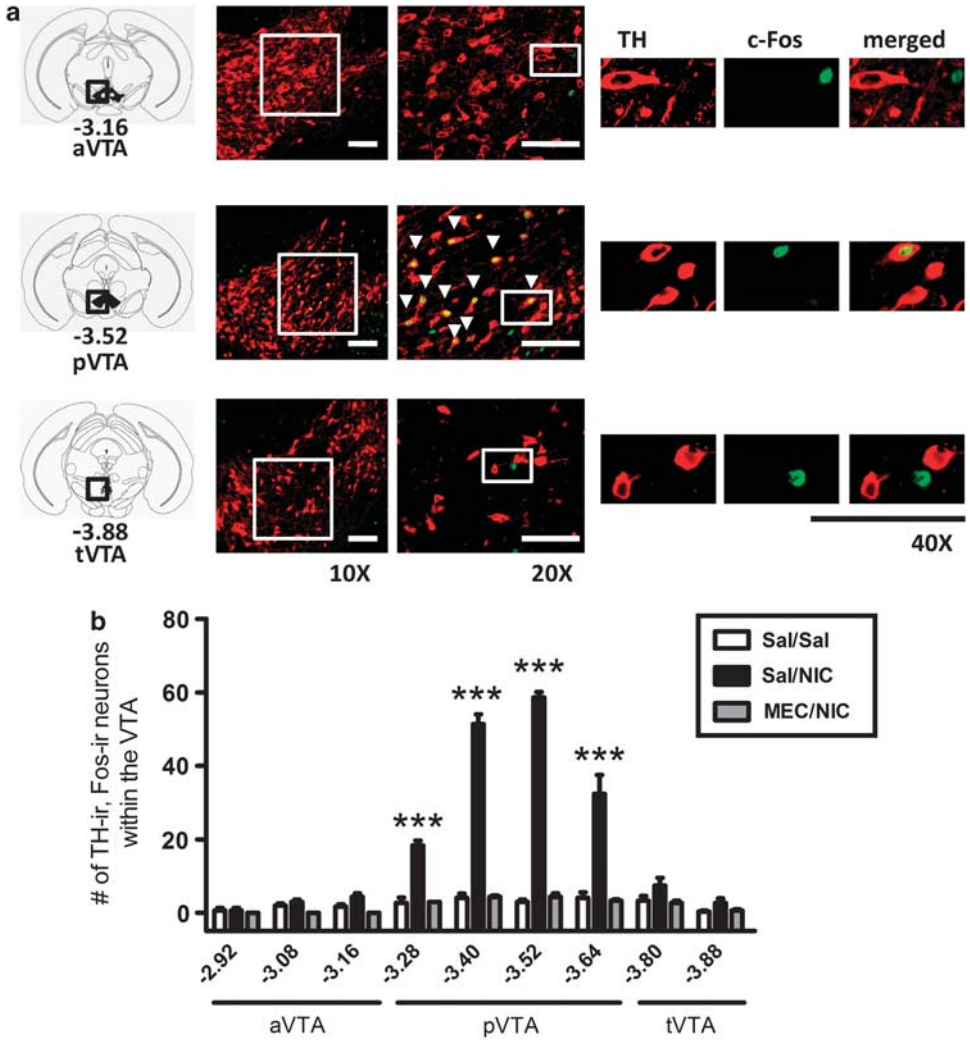

Figure 2 Nicotine selectively activates DAergic neurons within the pVTA. (a) Photomicrographs illustrating representative midbrain sections that include the aVTA (top), pVTA (middle), or tVTA (bottom) from C57Bl/6J mice injected with 0.5 mg/kg nicotine. Sections are immunolabeled for TH (red) and c-Fos (green). White boxes delineate slice regions that are magnified in the adjacent photomicrographs. White arrowheads point to neurons which are TH-ir, c-Fos-ir. Here, 40 × magnification images that illustrate labeling of TH (left), c-Fos (middle), and both (right), indicating nuclear localization of c-Fos in TH-expressing neurons are shown. Scale bar = 100 μm. (b) Number of TH-ir, c-Fos-ir neurons per VTA slice taken from mice administered two saline injections (Sal/Sal), a saline injection 15 min before a 0.5 mg/kg nicotine injection (Sal/NIC) or 3 mg/kg mecamylamine 15 min before nicotine (MEC/NIC). Distance from bregma is indicated on the *x* axis in millimeters. In all, 48 slices per treatment per mouse were analyzed ($n = 3$ mice per treatment). ***$p < 0.001$, compared with saline and mecamylamine treatment using two-way ANOVA and Bonferroni's post-test.

the number of neurons that were both TH-ir and c-Fos-ir (TH-ir, c-Fos-ir) compared with control animals. TH-ir, c-Fos-ir neurons were restricted to the pVTA (−3.28 to −3.64 mm from the bregma, Figure 2a and b). Preinjection of 3 mg/kg mecamylamine, a nonselective nAChR antagonist, 15 min before nicotine treatment, significantly reduced the number of TH-ir, c-Fos-ir neurons compared with a saline preinjection. There were no significant effects of treatment on the number of TH-ir, c-Fos-ir neurons within the aVTA or tVTA when compared with saline injection (Figure 2a and b). Nicotine also increased the number of TH-non-ir, c-Fos-ir neurons selectively in the pVTA, but the difference in the number of activated neurons compared with a saline injection was smaller than that of TH-ir neurons activated by nicotine (Supplementary Figure 1). Owing to the relatively small number of DAergic neurons present in the tVTA, we excluded this VTA subregion from further analysis. Acute nicotine could significantly activate aVTA DAergic neurons, but only at much higher doses. Thus, mice challenged with 2 mg/kg nicotine exhibited a significant increase in the number of TH-ir, c-Fos-ir aVTA neurons than did saline-injected animals (7.88 ± 1.38 per slice compared with 0.34 ± 0.09 per slice, respectively, $p < 0.01$, Supplementary Figure 2). Taken together, these data indicate that the rewarding, lower dose of nicotine selectively activates DAergic neurons in the pVTA.

Nicotine Directly Activates DAergic Neurons within the pVTA

To test the hypothesis that DAergic neurons within the pVTA are more sensitive to direct activation by nicotine than those in the aVTA, we measured DAergic neuron activity in adult (8–10 weeks) C57BL/6J midbrain slices in

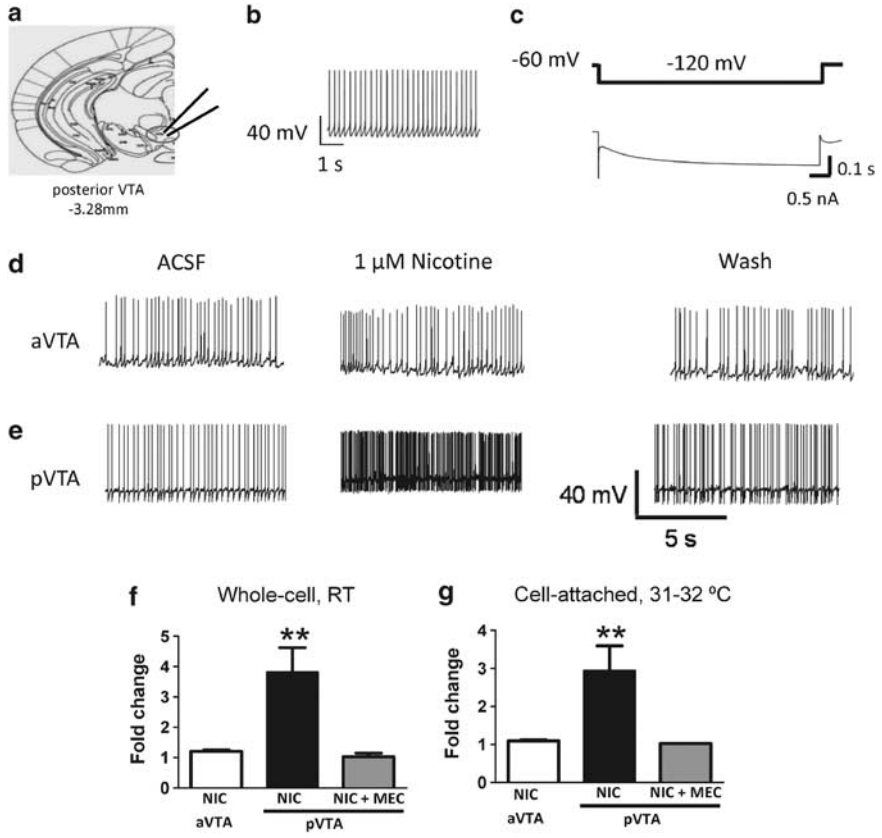

Figure 3 Direct activation of VTA DAergic neurons by nicotine. (a) Diagram of a mesocortical slice that includes the pVTA (red circle). Recordings were made from both pVTA and aVTA neurons. (b) Current-clamp ($I = 0$) trace illustrating the baseline firing frequency of a VTA DAergic neuron. (c) Whole-cell voltage clamp recording from a VTA neuron that expresses the hyperpolarization-activated cation current, I_h. The neuron was voltage clamped at −60 mV and hyperpolarized to −120 mV for 1.0 s before returning to the holding potential (Top). (d) Representative current-clamp ($I = 0$) recording from an aVTA DAergic neuron at baseline (ACSF, left), during application of 1 μM nicotine (middle, 3 min application), and after washout of nicotine (right). (e) Representative current-clamp ($I = 0$) recording from a pVTA DAergic neuron at baseline (ACSF, left), during application of 1 μM nicotine (middle, 3 min application), and after washout of nicotine (right). Burst firing upon washout (3–7 spikes per burst) was seen in 5 of 7 neurons with robust nicotine responses. (f) Summary of responses to nicotine in DAergic neurons from either the aVTA (white bar, $n = 8/8$) or the pVTA (black bar, $n = 7/16$). Each bar graph represents the fold change in action potential number produced by nicotine normalized to the baseline firing frequency. The response to nicotine in pVTA DAergic neurons was blocked by pre-exposure to 10 μM mecamylamine (gray bar). (g) Average response to nicotine as described in panel f ($n = 5$ neurons per region). Responses were recorded in cell-attached mode at 30–32°C. $^{**}p < 0.01$.

response to nicotine using whole-cell patch-clamp electrophysiology. DAergic neurons were identified based on expression of the hyperpolarization-activated cation current, I_h (Figure 3c), and baseline firing frequency (1–5 Hz, Figure 3b). In addition, after each recording, the content of the cell was aspirated into the patch pipette, and single-neuronal RT-PCR was performed to verify TH expression. DAergic neurons within the aVTA and the pVTA did not differ in resting membrane potential (−48.4 ± 2.7 mV and −52.7 ± 1.7 mV, respectively) input resistance (289.0 ± 43.0 MΩ and 317.9 ± 122.0 MΩ, respectively), or firing frequency (3.75 ± 1.5 Hz and 4.24 ± 0.52 Hz, respectively). To measure the direct activation by nicotine, we applied 1 μM of the drug, a concentration within the range of peak nicotine blood levels found in smokers (Henningfield *et al*, 1993; Russell *et al*, 1980). Nicotine was bath applied in the presence of a cocktail of inhibitors including CNQX, bicuculline, and atropine to block NMDA, GABAa, and muscarinic receptors, respectively. The firing frequency of DAergic neurons within the aVTA exhibited a small increase compared with baseline in response to nicotine (~1.2-fold, $n = 8/8$ neurons, Figure 3d and f). In contrast, 43.8% ($n = 7/16$) of DAergic neurons within the pVTA exhibited a robust increase in firing (~4-fold compared with baseline, Figure 3e and f) in response to nicotine, which was reversible upon washout and could be blocked by the noncompetitive nicotinic receptor antagonist, mecamylamine (10 μM). The remaining 9 out of 16 pVTA DAergic neurons had very small changes in firing frequency in response to nicotine (1.18 ± 0.08-fold compared with baseline). To ensure that DAergic neuron responses to nicotine were not artificially influenced by temperature or the whole-cell mode of recording, we also measured cell-attached nicotine-induced responses in VTA DAergic neurons in midbrain slices incubated at 31–32°C. Similar to room temperature whole-cell recordings, our cell-attached data revealed that nicotine had little effect on aVTA DAergic neuron activity, whereas nicotine increased DAergic neuron activity in the pVTA in all neurons tested (Figure 3g, 5/5 neurons). In addition, these responses were completely blocked by mecamylamine. Taken together, these data indicate that nicotine, at physiologically relevant concentrations, activated a subset of DAergic neurons within the pVTA, but not the aVTA.

Differential Expression of nAChR Subunit Genes in DAergic Neurons within the aVTA and the pVTA

To examine whether the region-selective activation of DAergic neurons by nicotine could be due to the differential expression of nAChRs between VTA subregions, we compared nicotinic receptor subunit gene expression between DAergic neurons in the aVTA and the pVTA. We collected TH-ir neurons within VTA subregions using LCM and quantified nAChR subunit gene expression by quantitative RT-PCR. In sum, the expression of nine nAChR subunit genes ($\alpha2$–$\alpha7$, $\beta2$–$\beta4$) was analyzed. In TH-ir neurons captured from the pVTA, the order of nAChR subunit gene expression, from highest to lowest expression was $\alpha4 > \beta3 > \alpha6 > \beta2 > \alpha7 > \alpha5 > \alpha3$ (Table 1). In TH-ir neurons captured from the aVTA, the order of expression, from highest to lowest expression was $\alpha4 > \beta3 > \alpha6 > \beta2 > \alpha7 > \alpha3 > \alpha5$ (Table 1). No $\alpha2$ or $\beta4$ gene expression was detected within either region (Table 1). A comparison of nAChR subunit gene expression in DAergic neurons of the aVTA and the pVTA expressed as fold change using the $2^{-\Delta\Delta Ct}$ method is illustrated in Figure 4. A paired *t*-test revealed significantly higher mRNA levels of the $\alpha4$ ($p<0.01$ for relative amplicon, $p<0.05$ for relative gene expression), $\alpha6$ ($p<0.05$, for both methods), and $\beta3$ genes ($p<0.05$, for both methods) in pVTA DAergic neurons than in aVTA DAergic neurons (Figure 4 and Table 1).

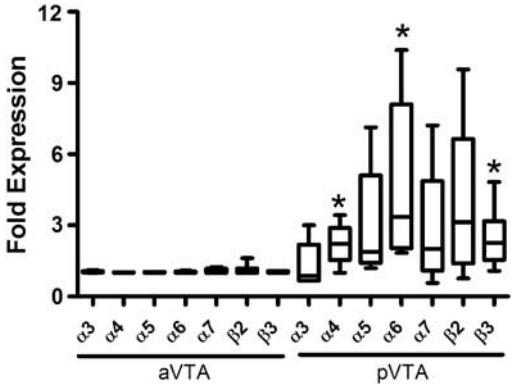

Figure 4 Differential expression of nAChR subunit genes in DAergic neurons within the aVTA and pVTA. TH-ir neurons from each region were collected by LCM, and nAChR expression was analyzed by qRT-PCR. A total of 23 104 and 23 886 of TH-ir neurons were collected from the aVTA and pVTA, respectively ($n=6$ mice per brain region). The line within each box plot represents the median difference of mRNA levels. The upper and lower edges of each box represent the 75th and the 25th percentile, respectively, whereas the upper and lower bars represent the maximum and minimum value, respectively. Expression of each subunit gene in the pVTA was compared with that in the aVTA using the $2^{-\Delta\Delta Ct}$ method. *$p<0.05$.

Nicotine Activates pVTA DAergic Neurons through α4* nAChRs

As (1) we found that $\alpha4$ subunit gene expression was highest within pVTA DAergic neurons and (2) that the activation of $\alpha4$* nAChRs is necessary and sufficient for nicotine dependence-related behaviors (Pons *et al*, 2008; Tapper *et al*, 2004), we tested the hypothesis that nicotine selectively activates pVTA DAergic neurons through $\alpha4$* nAChRs. We examined the effects of nicotine on c-Fos expression within TH-ir neurons in mice, which do not express $\alpha4$* nAChRs ($\alpha4$ KO), and mice expressing a single point mutation, Leu9′Ala, which renders $\alpha4$* nAChRs hypersensitive to agonist (Tapper *et al*, 2004).

Whereas 0.5 mg/kg nicotine significantly increased the number of TH-ir, c-Fos-ir neurons in the pVTA but not in

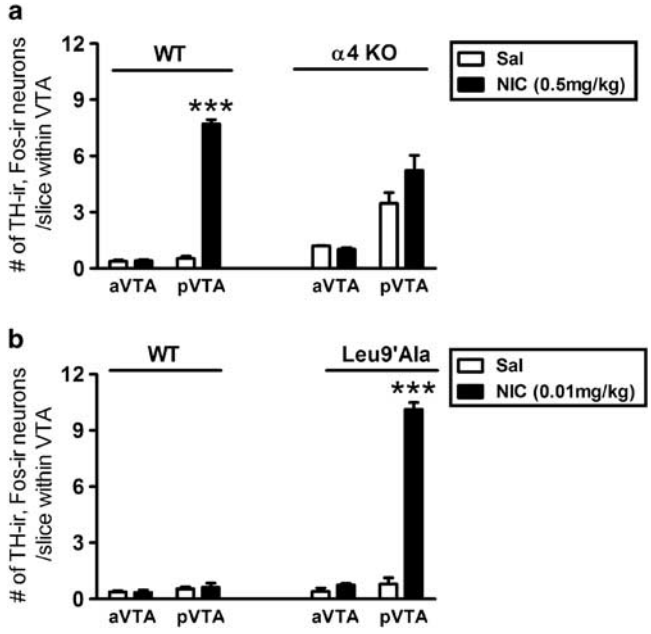

Figure 5 Activation of $\alpha4$* nAChRs is necessary and sufficient for nicotine activation of pVTA DAergic neurons. (a) Average number of TH-ir, c-Fos-ir neurons per slice from the aVTA or the pVTA (averaged regions as described in Figure 1) taken from WT (left) or $\alpha4$ KO mice receiving two saline injections (white bars) or saline, followed by a 0.5 mg/kg nicotine injection (black bars). (b) Average number of TH-ir, c-Fos-ir neurons per slice from the aVTA or the pVTA in WT or Leu9′Ala mice receiving two saline injections (white bars) or saline, followed by a 0.01 mg/kg nicotine injection (black bars). Cells were counted from 26 to 36 VTA slices per mouse. $n=3$ mice per treatment. ***$p<0.0001$. Bonferroni's post-test.

Table 1 Quantitative Gene Expression of nAChR Subunit Genes in DAergic Neurons of the aVTA or the pVTA

	α2	α3	α4**	α5	α6*	α7	β2	β3*	β4
aVTA	ND	−7.56 ± 0.47	−3.65 ± 0.37	−7.67 ± 1.18	−5.08 ± 1.14	−7.52 ± 1.14	−7.11 ± 0.61	−4.05 ± 0.58	n.d.
pVTA	ND	−7.49 ± 0.52	−2.61 ± 0.42	−6.62 ± 1.12	−3.39 ± 0.94	−6.58 ± 0.95	−5.68 ± 0.34	−2.94 ± 0.64	n.d.

Abbreviations: ND, not detectable.
Values represent the negative change in the threshold cycle ($^{-\Delta Ct}$) compared with GAPDH.
*$p<0.05$, **$p<0.01$, paired *T*-test.

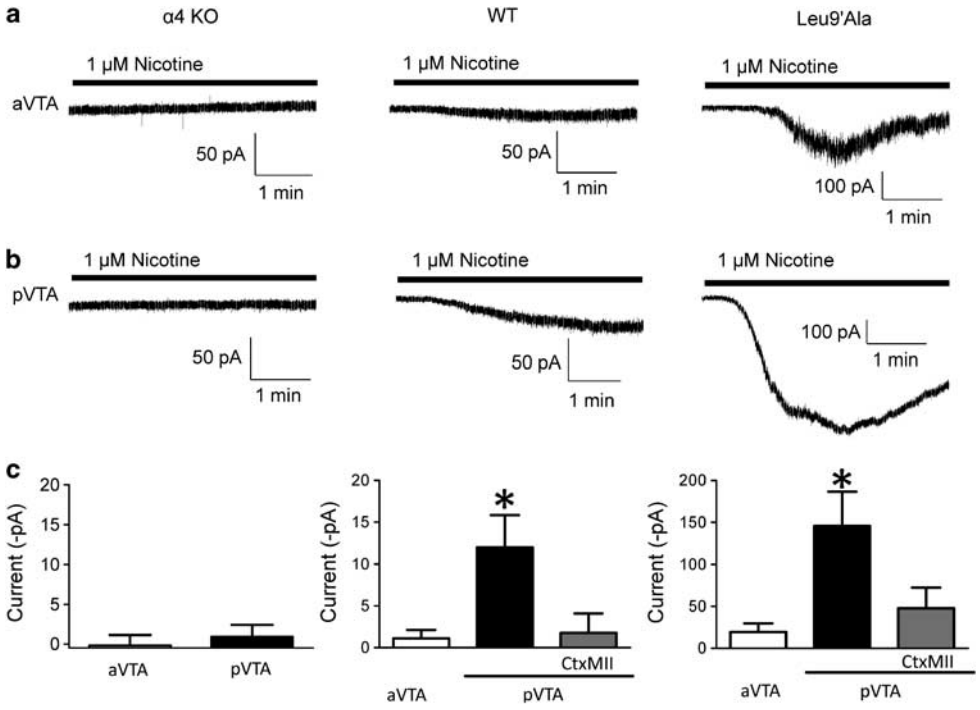

Figure 6 Response to nicotine in DAergic neurons under voltage clamp. Representative whole-cell responses to nicotine in (a) aVTA or (b) pVTA DAergic neurons from α4 KO (left), WT (middle), and Leu9′Ala mice. Neurons were held at −60 mV, and 1 μM nicotine was bath applied for 4 min. (c) Average peak responses to 1 μM nicotine in the aVTA (white bar) or pVTA (black bar) DAergic neurons from each mouse line. Peak responses typically occurred 2–3 min after initial nicotine application. The gray bar illustrates the average peak response to nicotine in pVTA DAergic neurons after 10 min application of 100 nM α-conotoxin MII (E11A). ($n = 7$ neurons per region per genotype). *$p < 0.05$.

the aVTA of WT mice (Figure 5a), there was less of an effect of the drug on α4 KO animals. We did observe elevated basal c-Fos expression in α4 KO mice likely reflecting the disinhibition of DAergic neurons in these animals as reported previously (Marubio *et al*, 2003). In KOs, two-way ANOVA revealed that there was a significant main effect of brain region ($F_{1,10} = 26.39$, $p < 0.001$), but no significant main effect of treatment (0.5 mg/kg nicotine, $F_{1,10} = 2.539$, $p = 0.142$) or brain region × treatment interaction ($F_{1,10} = 3.848$, $p = 0.078$). Thus, no significant differences were observed in the number of TH-ir, c-Fos-ir neurons between saline- and nicotine-injected animals either within the aVTA or within the pVTA (Figure 5a), indicating that the expression of α4* nAChRs is required for nicotine activation of pVTA DAergic neurons.

In response to 0.01 mg/kg nicotine, both WT aVTA and pVTA DAergic neurons were not activated by nicotine (Figure 5b). However, in Leu9′Ala mice, two-way ANOVA revealed that there was a significant main effect of brain region ($F_{1,9} = 173.1$, $p < 0.001$), treatment ($F_{1,9} = 189.6$, $p < 0.001$), and a significant brain region × treatment interaction ($F_{1,9} = 148.4$, $p < 0.001$). Thus, in contrast to α4 KO mice, Leu9′Ala mice challenged with a single injection of 0.01 mg/kg nicotine, the rewarding dose of nicotine in these animals (Tapper *et al*, 2004) and one that is 50-fold lower than the rewarding dose in WT mice, exhibited a significant and dramatic increase in the number of TH-ir, c-Fos-ir neurons within the pVTA ($p < 0.001$; Figure 5b) compared with saline-injected animals, whereas the aVTA was not affected (Figure 5b). Importantly, this low dose of nicotine did not activate DAergic neurons in WT animals, indicating that activation in the pVTA of Leu9′Ala mice by 0.01 mg/kg nicotine is due solely to activation of α4* nAChRs. Taken together, these data suggest that activation of α4* nAChRs is necessary and sufficient for nicotine-induced activation of DAergic neurons within the pVTA.

α4α6* nAChR-Binding Sites in the pVTA

On the basis of functional assays using striatal synaptosomes, α4α6* nAChRs have been shown to exhibit the highest sensitivity to nicotine of any nAChR to date (Salminen *et al*, 2007). To determine whether α4α6* nAChRs are expressed in the pVTA, we quantified α6* nAChR-binding sites in WT and α4 KO mice using the β2* nAChR radioligand, ^{125}I-A85380, in the presence and absence of the cold α6*-nAChR selective ligand, α-conotoxin MII. WT and α4 KO coronal sections spanning posterior regions of the VTA ($n = 6$ mice) were used for this analysis. In the absence of α-conotoxin MII, total binding was 8.82 ± 0.68 fmol/mg wet weight and 2.42 ± 0.20 fmol/mg wet weight in WT and α4 KO mice, respectively. In the presence of α-conotoxin MII, ^{125}I-A85380 binding was reduced to 7.43 ± 0.45 fmol/mg wet weight in WT mice and to 1.66 ± 0.76 fmol/mg wet weight in α4 KO mice. Thus, α-conotoxin MII-sensitive binding was reduced by 46% in α4 KO mice compared with WT mice (0.76 ± 0.23 fmol/mg wet weight compared with 1.39 ± 0.37 fmol/mg wet weight, respectively, Supplementary Figure 3). These data suggest that a portion of pVTA α6* nAChR-binding sites also contain the α4 subunit.

Whole-Cell Currents Induced by Nicotine in aVTA and pVTA DAergic Neurons

To test the hypothesis that selective activation of pVTA DAergic neurons by nicotine was directly mediated by increased functional α4* nAChR expression, we measured whole-cell currents induced by bath application of 1 μM nicotine in midbrain slices containing aVTA or pVTA DAergic neurons from α4 KO, WT, and Leu9′Ala mice. In WT mice, 1 μM nicotine induced whole-cell currents with a significantly larger peak response in the pVTA compared with aVTA DAergic neurons (Figure 6a–c, middle panels). In slices obtained from α4 KO mice, 1 μM nicotine did not elicit detectable currents in DAergic neurons from either VTA subregion (Figure 6a–c, left panels). Conversely, in slices obtained from Leu9′Ala mice, 1 μM nicotine elicited significant whole-cell currents in both aVTA and pVTA DAergic neurons (Figure 6a–c, right panels). However, the magnitude of current was significantly larger in pVTA DAergic neurons than in aVTA DAergic neurons. To test the hypothesis that the nicotine-induced currents we observed in pVTA DAergic neurons were mediated by α6* nAChRs, we tested the sensitivity of these currents to the α6 selective antagonist, α-conotoxin MII (E11A). Pretreatment with 100 nM α-conotoxin MII (E11A) significantly blocked whole-cell current in response to nicotine in pVTA DAergic neurons from WT and Leu9′Ala mice (Figure 6c, middle and right panels, respectively). These data indicate that the functional expression of α4* nAChRs is greater in pVTA DAergic neurons than in aVTA neurons and that these receptors also contain the α6 subunit.

Infusion of an α6 nAChR Selective Antagonist Blocks Nicotine Activation of pVTA DAergic Neurons

To gain insight into whether α6*-nAChRs are involved in nicotine activation of pVTA DAergic neurons *in vivo*, we infused vehicle or α-conotoxin MII (E11A) into the VTA of anesthetized WT mice before a challenge with 0.5 mg/kg nicotine and analyzed c-Fos expression in TH-ir neurons as a measure of DAergic neuron activation. Two-way ANOVA revealed that there was a significant main effect of brain region ($F_{1,14} = 205.2$, $p < 0.001$), treatment ($F_{2,14} = 56.71$, $p < 0.001$), and a significant brain region × treatment interaction ($F_{2,14} = 44.84$, $p < 0.001$, Figure 7a). Mice infused with α-conotoxin MII (E11A), followed by a 0.5 mg/kg nicotine i.p. injection exhibited a significant decrease in the number of TH-ir, c-Fos-ir neurons in the pVTA compared with animals that were infused with vehicle before a nicotine challenge (Figure 7a, $p < 0.001$). No significant differences were observed in the number of TH-ir, c-Fos-ir neurons between conotoxin and vehicle infusions within the aVTA (Figure 7a). In addition, infusion of α-conotoxin MII (E11A) followed by a saline injection did not significantly activate the VTA. These results indicate that α6*-nAChRs in the pVTA directly contribute to activation of pVTA DAergic neurons by nicotine.

Finally, to test the hypothesis that nAChRs containing both α4 and α6 subunits mediated the effects of nicotine on pVTA DAergic neurons *in vivo*, we selectively activated α4* nAChRs with 0.01 mg/kg nicotine in Leu9′Ala mice immediately after VTA infusion of either vehicle or α-conotoxin MII (E11A). Two-way ANOVA revealed that there was a significant main effect of brain region ($F_{1,12} = 240.4$, $p < 0.001$), treatment ($F_{2,12} = 87.18$, $p < 0.001$), and a significant brain region × treatment interaction ($F_{2,12} = 62.09$, $p < 0.001$). Leu9′Ala mice infused with α-conotoxin MII (E11A), followed by a 0.01 mg/kg nicotine i.p. injection exhibited a significant decrease in the number of TH-ir, c-Fos-ir neurons in the pVTA compared with animals that were infused with vehicle before a nicotine challenge ($p < 0.001$, Figure 7b). No significant differences were observed in the number of TH-ir, c-Fos-ir neurons between conotoxin and vehicle infusions within the aVTA (Figure 7b). As in WT mice, infusion of α-conotoxin MII (E11A) followed by a saline injection did not significantly activate the VTA. These results indicate that α4α6* nAChRs in the pVTA directly contribute to activation of DAergic neurons by nicotine.

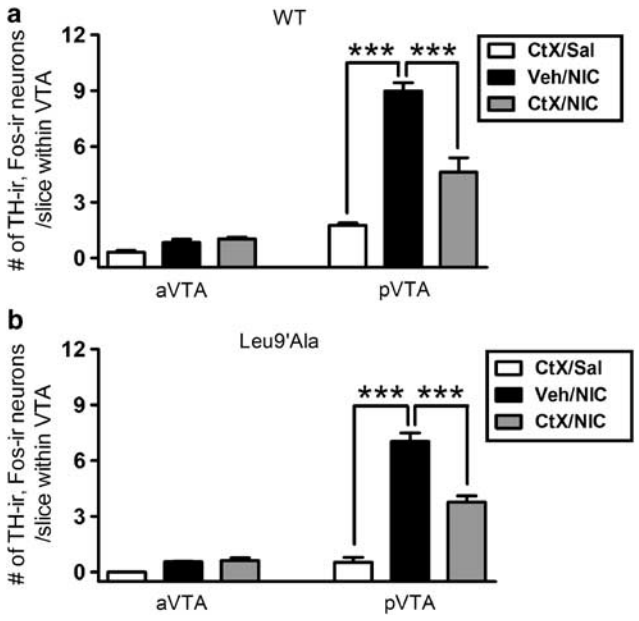

Figure 7 Effect of VTA infusion of an α6* nAChR antagonist on nicotine-induced VTA DAergic neuron activation. (a) Average number of TH-ir, c-Fos-ir neurons in the aVTA and the pVTA (averaged regions as described in Figure 1) from WT mice receiving VTA infusion of vehicle (black bar) or α-conotoxin MII (E11A) (gray bar), followed by a 0.5 mg/kg nicotine injection. Control mice received infusion of 100 nM conotoxin MII (E11A), followed by a saline injection. (b) Average number of TH-ir, c-Fos-ir neurons in the aVTA and pVTA (averaged regions as described in Figure 1) from Leu9′Ala mice receiving VTA infusion of vehicle (black bar), or 100 nM α-conotoxin MII (E11A) infusion (gray bar), followed by a 0.01 mg/kg nicotine injection. Control mice received infusion of conotoxin MII (E11A), followed by a saline injection. Cells were counted from 25 to 34 VTA slices per mouse ($n = 3$–4 mice per treatment). ***$p < 0.001$.

DISCUSSION

Emerging evidence indicates that the VTA is not a homogenous brain structure; rather it can be divided into at least three subregions including anterior, posterior, and tail (Ikemoto, 1998, 2007; Olson *et al*, 2005; Zangen *et al*, 2002). The aVTA and pVTA subregions respond differently

to drugs of abuse, including opiates and alcohol (Boehm *et al*, 2002; Ericson *et al*, 2008; Rodd *et al*, 2004, 2005; Shabat-Simon *et al*, 2008). Supporting this hypothesis, Figure 1 illustrates that DAergic neurons within the aVTA, pVTA, and tVTA differ in size distribution and density, suggesting that distinct populations of DAergic neurons may exist. This is consistent with recent studies indicating that, in primates, individual DAergic neurons within the VTA differentially respond to rewarding or aversive stimuli (Matsumoto and Hikosaka, 2009). Furthermore, nicotine, at rewarding doses, selectively activates DAergic neurons within the pVTA and does not activate the aVTA or the tVTA. Activation of pVTA DAergic neurons is dependent on nAChR activation because preinjection of the non-competitive nAChR antagonist, mecamylamine, completely blocked activation. Thus, DAergic neurons specifically within the pVTA are likely critical for nicotine reinforcement. These data support previous studies, indicating that rats will self-administer nicotine directly into the posterior, but not into the aVTA (Ikemoto *et al*, 2006). Nicotine can activate DAergic neurons within the aVTA but only at a high, extraphysiological dose near the seizure-inducing threshold for C57BL/6J mice (Fonck *et al*, 2005).

Our data from midbrain slices indicate that pVTA DAergic neurons are more sensitive to direct activation by 1 μM nicotine compared with those in aVTA, suggesting that nAChR sensitivity differs between regions. This concentration of nicotine is within the range found in smokers' blood (Henningfield *et al*, 1993; Russell *et al*, 1980) and was bath applied to slices. As nicotine-induced desensitization of nAChRs occurs rapidly (Mansvelder *et al*, 2002a; Mansvelder and McGehee, 2002b), we cannot rule out the possibility that smaller responses to nicotine in DAergic neurons are caused by nAChR desensitization. However, bath application of nicotine more accurately mimics exposure from cigarette smoke, and our data indicate that DAergic neurons only within the pVTA are robustly activated by nicotine. This result was independent of temperature or mode of recording, although the response to nicotine in the pVTA was more consistent in a cell-attached mode in which the integrity of the recorded neurons was retained. Previous studies have examined nicotine activation of DAergic neurons in midbrain slices, and our data are consistent with these studies in that (1) bath application of nicotine can directly activate these neurons and (2) responses to nicotine in DAergic neurons are variable likely reflecting multiple DAergic populations that express distinct nAChR subtypes (Dani *et al*, 2000; Fisher *et al*, 1998; Klink *et al*, 2001; Pidoplichko *et al*, 1997; Wooltorton *et al*, 2003). It is important to point out that the majority of studies using electrophysiology to analyze nicotine effects on VTA DAergic neurons in midbrain slice have used young (ie, mostly 12–25-day-old) animals and did not analyze VTA subregions in detail.

Taken together, our immunohistochemical and biophysical analyses suggest that DAergic neurons within the aVTA and pVTA may express distinct nAChR subtypes, which could explain the differential response to nicotine. This also supports a recent study that identified three distinct whole-cell current responses to nicotine in acutely dissociated VTA DAergic neurons (Yang *et al*, 2009). Indeed, DAergic neurons within the pVTA exhibited a significantly higher expression of α4, α6, and β3 subunit genes than did DAergic neurons in the aVTA. Several studies have analyzed nAChR expression in the VTA and substantia nigra pars compacta, and our data are in general agreement that expressions of α4, α6, β2, and β3 nAChR subunit genes are abundant in DAergic neurons (Klink *et al*, 2001; Wooltorton *et al*, 2003).

Our results indicate that activation of α4* nAChRs is necessary and sufficient for activation of pVTA DAergic neurons. Analysis of c-Fos induction in DAergic neurons indicated that nicotine failed to activate pVTA DAergic neurons in α4 KO mice, whereas selective activation of α4* nAChRs with low doses of nicotine in Leu9′Ala mice was sufficient to activate pVTA DAergic neurons. In midbrain slices, DAergic neurons within the pVTA exhibited larger nicotine-induced whole-cell current than did aVTA DAergic neurons, indicating that the observed increase in subunit gene transcripts was also reflected in greater functional expression of nAChRs. Indeed, functional nAChRs activated by 1 μM nicotine in pVTA DAergic neurons contained the α4 subunit because nicotine-induced current was not observed in α4 KO mice. In addition, pVTA DAergic neurons exhibited larger nicotine-induced whole-cell current than did aVTA DAergic neurons recorded from Leu9′Ala mice supporting the contribution of α4* nAChRs to the nicotine response in pVTA neurons.

In WT mice, α6* nAChRs also contributed to nicotine activation of pVTA DAergic neurons as infusion of α-conotoxin MII (E11A) into the VTA significantly blocked activation. These data are in agreement with a recent study indicating that VTA infusion of α-conotoxin MII blocks nicotine-induced DA release into the NAc and also blocks nicotine self-administration in rats (Gotti *et al*, 2010). Although conotoxin infusion significantly blocked nicotine activation of the pVTA, it was not complete. Thus, we cannot rule out the possibility that other mechanisms, such as nicotine-mediated glutamate release, may also contribute to activation of this brain region (Kenny *et al*, 2009; Mansvelder *et al*, 2002a). However, consistent with our immunohistochemical and gene expression data, nicotine-induced currents in WT pVTA DAergic neurons were also blocked by α-conotoxin MII (E11A) indicating a direct effect of nicotine by activation of α6* nAChRs expressed in DAergic neurons.

Importantly, at least two subtypes of α6* nAChRs have been identified, α6 (non-α4) β2* and α6α4β2* nAChRs, the latter subtype being the most nicotine-sensitive receptor identified to date (Grady *et al*, 2007; Salminen *et al*, 2007). The identity and functional role of these nAChR subtypes have been elucidated predominantly using striatal synaptosomes, and our studies extend these observations to DAergic neurons within the pVTA. Our radioligand-binding data indicate that a portion of α6* nAChR-binding sites also contain the α4 subunit. In addition, nicotine-induced currents in DAergic neurons were dependent on α4* nAChR expression and blocked by α-conotoxin MII (E11A) in both WT and Leu9′Ala midbrain slices, indicating functional expression of α4α6* nAChRs in the VTA. Finally, selective activation of pVTA DAergic neurons in Leu9′Ala mice using a small dose of nicotine that has no effect in WT mice, was also blocked by VTA infusion of α-conotoxin MII (E11A). These data provide the first direct evidence that functional α4α6* nAChRs contribute to nicotine-mediated activation of

pVTA DAergic neurons. Although α4* nAChRs are a predominant subtype expressed throughout the VTA, functional α4α6* nAChRs are enriched in pVTA DAergic neurons, such that these neurons are activated by lower concentrations of nicotine compared with DAergic neurons in other subregions of the VTA. Thus, our data, in combination with the recent study by Gotti *et al* (2010) indicate that α6α4β2* nAChRs expressed in DAergic neurons of the pVTA mediate the reinforcing properties of nicotine.

Taken together, our data indicate that, at rewarding doses, nicotine selectively activates DAergic neurons within the posterior subregion of the VTA through α4α6* nAChRs. These receptors could provide a novel molecular target for smoking-cessation therapeutics.

ACKNOWLEDGEMENTS

This study was supported by the National Institute On Alcohol Abuse and Alcoholism award numbers R01AA017656 and R21AA018042 (ART), the National Institute of Mental Health R01MH53631 (JMM), the National Institute on Drug Abuse award numbers DA003194 (MJM) and DA012242 (MJM and JMM), and the National Institute on Neurological Disorders and Stroke award number R01NS030243 (PDG). The content is solely the responsibility of the authors and does not necessarily represent the official views of the National Institute on Alcohol Abuse and Alcoholism, the National Institute on Drug Abuse, the National Institute on Neurological Disorders and Stroke, or the National Institutes of Health.

DISCLOSURE

The authors declare no conflict of interest.

REFERENCES

Albuquerque EX, Pereira EF, Alkondon M, Rogers SW (2009). Mammalian nicotinic acetylcholine receptors: from structure to function. *Physiol Rev* **89**: 73–120.

Boehm II SL, Piercy MM, Bergstrom HC, Phillips TJ (2002). Ventral tegmental area region governs GABA(B) receptor modulation of ethanol-stimulated activity in mice. *Neuroscience* **115**: 185–200.

CDC (2010). Vital signs: current cigarette smoking among adults aged ⩾18 years—United States, 2009. *MMWR Morb Mortal Wkly Rep* **59**: 1135–1140.

Champtiaux N, Gotti C, Cordero-Erausquin M, David DJ, Przybylski C, Lena C *et al* (2003). Subunit composition of functional nicotinic receptors in dopaminergic neurons investigated with knock-out mice. *J Neurosci* **23**: 7820–7829.

Champtiaux N, Han ZY, Bessis A, Rossi FM, Zoli M, Marubio L *et al* (2002). Distribution and pharmacology of alpha 6-containing nicotinic acetylcholine receptors analyzed with mutant mice. *J Neurosci* **22**: 1208–1217.

Cole AJ, Saffen DW, Baraban JM, Worley PF (1989). Rapid increase of an immediate early gene messenger RNA in hippocampal neurons by synaptic NMDA receptor activation. *Nature* **340**: 474–476.

Dani JA (2003). Roles of dopamine signaling in nicotine addiction. *Mol Psychiatry* **8**: 255–256.

Dani JA, Radcliffe KA, Pidoplichko VI (2000). Variations in desensitization of nicotinic acetylcholine receptors from hippocampus and midbrain dopamine areas. *Eur J Pharmacol* **393**: 31–38.

Ericson M, Lof E, Stomberg R, Chau P, Soderpalm B (2008). Nicotinic acetylcholine receptors in the anterior, but not posterior, ventral tegmental area mediate ethanol-induced elevation of accumbal dopamine levels. *J Pharmacol Exp Ther* **326**: 76–82.

Fisher JL, Pidoplichko VI, Dani JA (1998). Nicotine modifies the activity of ventral tegmental area dopaminergic neurons and hippocampal GABAergic neurons. *J Physiol Paris* **92**: 209–213.

Fonck C, Cohen BN, Nashmi R, Whiteaker P, Wagenaar DA, Rodrigues-Pinguet N *et al* (2005). Novel seizure phenotype and sleep disruptions in knock-in mice with hypersensitive alpha 4* nicotinic receptors. *J Neurosci* **25**: 11396–11411.

Gotti C, Guiducci S, Tedesco V, Corbioli S, Zanetti L, Moretti M *et al* (2010). Nicotinic acetylcholine receptors in the mesolimbic pathway: primary role of ventral tegmental area alpha6beta2* receptors in mediating systemic nicotine effects on dopamine release, locomotion, and reinforcement. *J Neurosci* **30**: 5311–5325.

Grady SR, Salminen O, Laverty DC, Whiteaker P, McIntosh JM, Collins AC *et al* (2007). The subtypes of nicotinic acetylcholine receptors on dopaminergic terminals of mouse striatum. *Biochem Pharmacol* **74**: 1235–1246.

Hendrickson LM, Zhao-Shea R, Tapper AR (2009). Modulation of ethanol drinking-in-the-dark by mecamylamine and nicotinic acetylcholine receptor agonists in C57BL/6J mice. *Psychopharmacology (Berl)* **204**: 563–572.

Henningfield JE, Stapleton JM, Benowitz NL, Grayson RF, London ED (1993). Higher levels of nicotine in arterial than in venous blood after cigarette smoking. *Drug Alcohol Depend* **33**: 23–29.

Hokfelt T, Everitt BJ, Theodorsson-Norheim E, Goldstein M (1984a). Occurrence of neurotensinlike immunoreactivity in subpopulations of hypothalamic, mesencephalic, and medullary catecholamine neurons. *J Comp Neurol* **222**: 543–559.

Hokfelt T, Johansson O, Goldstein M (1984b). Chemical anatomy of the brain. *Science* **225**: 1326–1334.

Ikemoto S (2007). Dopamine reward circuitry: two projection systems from the ventral midbrain to the nucleus accumbens-olfactory tubercle complex. *Brain Res Rev* **56**: 27–78.

Ikemoto S, Murphy JM, McBride WJ (1998). Regional differences within the rat ventral tegmental area for muscimol self-infusions. *Pharmacol Biochem Behav* **61**: 87–92.

Ikemoto S, Qin M, Liu ZH (2006). Primary reinforcing effects of nicotine are triggered from multiple regions both inside and outside the ventral tegmental area. *J Neurosci* **26**: 723–730.

Ikemoto S, Wise RA (2002). Rewarding effects of the cholinergic agents carbachol and neostigmine in the posterior ventral tegmental area. *J Neurosci* **22**: 9895–9904.

Kaufling J, Veinante P, Pawlowski SA, Freund-Mercier MJ, Barrot M (2009). Afferents to the GABAergic tail of the ventral tegmental area in the rat. *J Comp Neurol* **513**: 597–621.

Kenny PJ, Chartoff E, Roberto M, Carlezon Jr WA, Markou A (2009). NMDA receptors regulate nicotine-enhanced brain reward function and intravenous nicotine self-administration: role of the ventral tegmental area and central nucleus of the amygdala. *Neuropsychopharmacology* **34**: 266–281.

Klink R, de Kerchove d'Exaerde A, Zoli M, Changeux JP (2001). Molecular and physiological diversity of nicotinic acetylcholine receptors in the midbrain dopaminergic nuclei. *J Neurosci* **21**: 1452–1463.

Laviolette SR, van der Kooy D (2004). The neurobiology of nicotine addiction: bridging the gap from molecules to behaviour. *Nat Rev Neurosci* **5**: 55–65.

Mansvelder HD, Keath JR, McGehee DS (2002a). Synaptic mechanisms underlie nicotine-induced excitability of brain reward areas. *Neuron* **33**: 905–919.

Mansvelder HD, McGehee DS (2002b). Cellular and synaptic mechanisms of nicotine addiction. *J Neurobiol* **53**: 606–617.

Marubio LM, Gardier AM, Durier S, David D, Klink R, Arroyo-Jimenez MM *et al* (2003). Effects of nicotine in the dopaminergic system of mice lacking the alpha4 subunit of neuronal nicotinic acetylcholine receptors. *Eur J Neurosci* **17**: 1329–1337.

Maskos U, Molles BE, Pons S, Besson M, Guiard BP, Guilloux JP *et al* (2005). Nicotine reinforcement and cognition restored by targeted expression of nicotinic receptors. *Nature* **436**: 103–107.

Matsumoto M, Hikosaka O (2009). Two types of dopamine neuron distinctly convey positive and negative motivational signals. *Nature* **459**: 837–841.

McIntosh JM, Azam L, Staheli S, Dowell C, Lindstrom JM, Kuryatov A *et al* (2004). Analogs of alpha-conotoxin MII are selective for alpha6-containing nicotinic acetylcholine receptors. *Mol Pharmacol* **65**: 944–952.

National Research Council (1996). *Guide for the Care and use of Laboratory Animals*. National Academy Press: Washington, DC.

Olson VG, Zabetian CP, Bolanos CA, Edwards S, Barrot M, Eisch AJ *et al* (2005). Regulation of drug reward by cAMP response element-binding protein: evidence for two functionally distinct subregions of the ventral tegmental area. *J Neurosci* **25**: 5553–5562.

Paxinos G, Franklin K (2000). *The Mouse Brain in Stereotaxic Coordinates* 2nd edn. Academic Press: San Diego, CA. p 296.

Perrotti LI, Bolanos CA, Choi KH, Russo SJ, Edwards S, Ulery PG *et al* (2005). DeltaFosB accumulates in a GABAergic cell population in the posterior tail of the ventral tegmental area after psychostimulant treatment. *Eur J Neurosci* **21**: 2817–2824.

Picciotto MR, Zoli M, Rimondini R, Lena C, Marubio LM, Pich EM *et al* (1998). Acetylcholine receptors containing the beta2 subunit are involved in the reinforcing properties of nicotine. *Nature* **391**: 173–177.

Pidoplichko VI, DeBiasi M, Williams JT, Dani JA (1997). Nicotine activates and desensitizes midbrain dopamine neurons. *Nature* **390**: 401–404.

Pons S, Fattore L, Cossu G, Tolu S, Porcu E, McIntosh JM *et al* (2008). Crucial role of alpha4 and alpha6 nicotinic acetylcholine receptor subunits from ventral tegmental area in systemic nicotine self-administration. *J Neurosci* **28**: 12318–12327.

Rodd ZA, Bell RL, Zhang Y, Murphy JM, Goldstein A, Zaffaroni A *et al* (2005). Regional heterogeneity for the intracranial self-administration of ethanol and acetaldehyde within the ventral tegmental area of alcohol-preferring (P) rats: involvement of dopamine and serotonin. *Neuropsychopharmacology* **30**: 330–338.

Rodd ZA, Melendez RI, Bell RL, Kuc KA, Zhang Y, Murphy JM *et al* (2004). Intracranial self-administration of ethanol within the ventral tegmental area of male Wistar rats: evidence for involvement of dopamine neurons. *J Neurosci* **24**: 1050–1057.

Ross SA, Wong JY, Clifford JJ, Kinsella A, Massalas JS, Horne MK *et al* (2000). Phenotypic characterization of an alpha 4 neuronal nicotinic acetylcholine receptor subunit knock-out mouse. *J Neurosci* **20**: 6431–6441.

Russell MA, Jarvis M, Iyer R, Feyerabend C (1980). Relation of nicotine yield of cigarettes to blood nicotine concentrations in smokers. *Br Med J* **280**: 972–976.

Salminen O, Drapeau JA, McIntosh JM, Collins AC, Marks MJ, Grady SR (2007). Pharmacology of alpha-conotoxin MII-sensitive subtypes of nicotinic acetylcholine receptors isolated by breeding of null mutant mice. *Mol Pharmacol* **71**: 1563–1571.

Shabat-Simon M, Levy D, Amir A, Rehavi M, Zangen A (2008). Dissociation between rewarding and psychomotor effects of opiates: differential roles for glutamate receptors within anterior and posterior portions of the ventral tegmental area. *J Neurosci* **28**: 8406–8416.

Tapper AR, McKinney SL, Nashmi R, Schwarz J, Deshpande P, Labarca C *et al* (2004). Nicotine activation of alpha4* receptors: sufficient for reward, tolerance, and sensitization. *Science* **306**: 1029–1032.

Tapper AR, Nashmi R, Lester HA (2006). Neuronal nicotinic acetylcholine receptors and nicotine dependence. *Cell Biology of Addiction*. Cold Spring Harbor Laboratory Press: Cold Spring, Harbor, NY. pp 179–191.

Wooltorton JR, Pidoplichko VI, Broide RS, Dani JA (2003). Differential desensitization and distribution of nicotinic acetylcholine receptor subtypes in midbrain dopamine areas. *J Neurosci* **23**: 3176–3185.

Yang K, Hu J, Lucero L, Liu Q, Zheng C, Zhen X *et al* (2009). Distinctive nicotinic acetylcholine receptor functional phenotypes of rat ventral tegmental area dopaminergic neurons. *J Physiol* **587**(Part 2): 345–361.

Zangen A, Ikemoto S, Zadina JE, Wise RA (2002). Rewarding and psychomotor stimulant effects of endomorphin-1: anteroposterior differences within the ventral tegmental area and lack of effect in nucleus accumbens. *J Neurosci* **22**: 7225–7233.

Zangen A, Solinas M, Ikemoto S, Goldberg SR, Wise RA (2006). Two brain sites for cannabinoid reward. *J Neurosci* **26**: 4901–4907.

Supplementary Information accompanies the paper on the Neuropsychopharmacology website (http://www.nature.com/npp)